CONNECTIONS BETWEEN THE WHITE-LIGHT ECLIPSE CORONA AND MAGNETIC FIELDS OVER THE SOLAR CYCLE

J. SÝKORA[1], O. G. BADALYAN[2] and V. N. OBRIDKO[2]
[1]*Astronomical Institute of the Slovak Academy of Sciences, 05960 Tatranská Lomnica, Slovak Republic (e-mail: sykora@ta3.sk)*
[2]*Institute of Terrestrial Magnetism, Ionosphere and Radio Wave Propagation, 142190 Troitsk, Russia (e-mail: badalyan@izmiran.troitsk.ru)*

(Received 27 May 2002; accepted 27 September 2002)

Abstract. Observations of ten solar eclipses (1973–1999) enabled us to reveal and describe mutual relations between the white-light corona structures (e.g., global coronal forms and most conspicuous coronal features, such as helmet streamers and coronal holes) and the coronal magnetic field strength and topology. The magnetic field strength and topology were extrapolated from the photospheric data under the current-free assumption. In spite of this simplification the found correspondence between the white-light corona structure and magnetic field organization strongly suggests a governing role of the field in the appearance and evolution of local and global structures. Our analysis shows that the study of white-light corona structures over a long period of time can provide valuable information on the magnetic field cyclic variations. This is particularly important for the epoch when the corresponding measurements of the photospheric magnetic field are absent.

1. Introduction

The life of the solar corona is mostly governed by the magnetic field. In fact, the global and large-scale magnetic fields control and order the distribution of the whole matter in the corona. The strength and organization of those fields clearly foreordain the presence of different coronal structures (coronal streamers, holes, plumes, condensations, etc.), the global form of the eclipse corona, and the position and shape of the heliospheric current sheet.

In fact, no direct measurements of the coronal magnetic field exist nowadays, so the magnetic field between the photosphere and the source surface is difficult to study. The only available methods are based on theoretical calculations of the coronal magnetic field under some simplifying assumptions, e.g., the potential or, sometimes, force-free character of the magnetic field. An estimate of the magnetic field strength may be obtained from radio data, also under a certain assumption of the radiation mechanism (see, e.g., Gelfreikh, Pilyeva, and Ryabov, 1997; Grebinskij *et al.*, 2000). Besides, the radio measurements allow the magnetic field to be estimated in the regions of the strongest field only, basically, above the sunspot regions.

A close relationship between the solar magnetic field and the coronal structure enables a better understanding of the coronal magnetic field. Investigation of the

Solar Physics **212:** 301–318, 2003.

large-scale coronal magnetic field and its cyclic variations seems to be particularly promising. To approach this task, the relation between the white-light corona and magnetic field during the solar cycle should be understood.

The present-day knowledge on the solar corona comes basically from the space-borne instruments of the *Yohkoh*, SOHO, and TRACE missions. The X-ray measurements make it possible to study the fine structure of the inner corona. The SOHO LASCO coronagraphs provide images in the range of 2–30 $R_\odot$, allowing the individual streamers to be investigated up to these large distances. The range between 1 and 2 $R_\odot$ remains mostly uncovered by the white-light corona observations from space. On the other hand, this is the range for which the coronal magnetic field can be derived most reliably. One should also notice that the white-light corona observations from space only partly cover solar cycles 22 and 23.

The photographic observations of white-light corona performed during solar eclipses date back to the second half of the 19th century. The global shape of the corona and its cyclic evolution were described by many authors in the past, and rather complete catalogues of the coronal structure drawings were published (Vsekhsvyatsky *et al.*, 1965; Loucif, 1988; Loucif and Koutchmy, 1989).

Systematic measurements of the photospheric magnetic fields performed with sufficiently good space resolution and covering the whole Sun's disk (necessary for calculations of the coronal magnetic field) are available from the beginning of cycle 21. Prior to that period, the magnetic data exist for the end of cycle 19 and the entire cycle 20. However, these are the data from different observatories obtained using different measuring procedures. Their reduction to one scale is a non-trivial task (Obridko and Shelting, 1999a). For even earlier periods, back to 1880, the magnetic field can be 'reconstructed' with a certain degree of reliability from the Hα charts and prominences (Vasil'eva, 1998; Vasil'eva and Tlatov, 2002). In doing this, we only determine the field polarity in the photosphere and lower chromosphere.

It is evident that by analysing the coronal structures and the general form of the corona recorded during a certain eclipse we are able to say a lot about the magnetic field. The present paper is aimed in that direction.

Our observations cover the time interval from 1973 to 1999, when ten solar eclipses were successfully recorded. Nine of them fall in the period for which reliably homogeneous measurements of the photospheric magnetic field are available (Wilcox Solar Observatory, *http://quake.stanford.edu*). Magnetic field data for the 1973 eclipse were obtained from Mount Wilson Observatory measurements. All ten eclipses were observed and processed by nearly the same method yielding a sufficiently uniform final data set. The last three eclipses (1997, 1998, and 1999) belong to the ascending phase of the current cycle 23, which is now intensively studied.

The eclipse observations and measurements usually included obtaining the white-light corona images and the polarized images in the continuum and in the brightest optical coronal emission line Fe XIV 530.3 nm (the so-called coronal

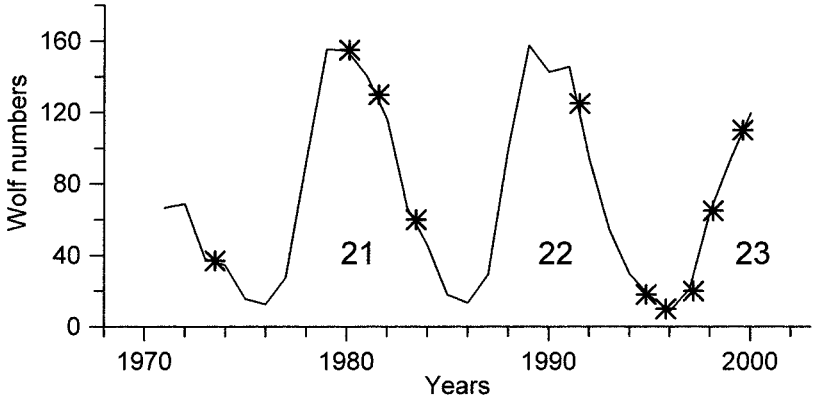

Figure 1. Positions of the observed eclipses (*asterisks*) on the curve of the yearly Wolf numbers. Numbers of the sunspot cycles are denoted.

green line). In general, we have investigated two topics: (a) connection of the large-scale white-light corona structures with the calculated magnetic field on the eclipse days and evolution of the general coronal form with the phase of the solar cycle and (b) interpretation of the polarization measurements in connection with the magnetic type of the corresponding large-scale coronal structure (coronal streamers, coronal holes, polar plumes). Some results of our study are published in (concerning (a)) Sýkora *et al.* (1998, 1999) and Sýkora, Badalyan, and Obridko (2002) and (concerning (b)) Badalyan and Sýkora (1997), Badalyan, Livshits, and Sýkora (1997, 1999), Badalyan, Obridko, and Sýkora (2002a, b).

The present paper considers all the ten solar eclipses with a goal to provide a general picture of close relationship between the structures, quantities, and evolution of both the white-light corona and the coronal magnetic field, emphasizing the governing role of the field in this relationship. To fulfill this task, different ways of representing the magnetic field have been used: the synoptic charts, 3D-distribution of the open and closed field lines on the Sun's surface, and isolines of the magnetic field strength in the plane of the sky. The full set of data at our disposal allows us to determine what basic harmonics of the magnetic field describe best the white-light corona shape. In principle, relying on the structural coronal drawings, the main characteristics of the solar magnetic field could be determined in the past.

2. Observational Data and Procedure of Calculations

The initial information on the ten solar eclipses we observed during 1973–1999 is given in Table I and Figure 1. Namely, the date, place of observation, phase Φ in the cycle, and flattening of the solar corona are presented. According to Mitchell (1929), for each of the eclipses $\Phi = (T - m)/(|M - m|)$, where T is date of the eclipse and M and m are the dates of the cycle maximum and minimum,

TABLE I
List of the eclipses observed (1973–1999).

No.	Date	Place	Cycle phase	Flattening
1	1973 (30 June)	El Meki, Rep. of Niger	−0.41	0.239
2	1980 (16 Feb.)	Jawalagera, India	−0.95	0.016
3	1981 (31 July)	Tarma (Bratsk), U.S.S.R.	−0.76	0.187
4	1983 (11 June)	Cepù, Indonesia	−0.39	0.251
5	1991 (11 July)	La Paz, Mexico	−0.75	0.002
6	1994 (3 Nov.)	Criciùma, Brazil	−0.33	0.142
7	1995 (24 Oct.)	Nakhon Sawan, Thailand	−0.16	0.159
8	1997 (9 March)	Pervomajskij, Russia	+0.14	0.207
9	1998 (26 Feb.)	Gros Cap, Guadeloupe	+0.41	0.215
10	1999 (11 Aug.)	Tihany, Hungary	+0.82	0.037

respectively. The coronal flattening ε was derived by the definition of Ludendorff (1928).

The coronal magnetic field was calculated under the potential field approximation from the longitudinal field component measured by Wilcox Solar Observatory at the level of the photosphere. Some details about our calculations can be also found in Ivanov and Kharshiladze (1994) and Sýkora *et al.* (1999).

In the present paper, the strength of the magnetic field B and its components are calculated and analysed. We have constructed the synoptic charts of the radial component B_r, as derived for the source surface level. On these charts, the magnetic neutral line (representing the magnetic equator as the basis of the heliospheric current sheet) and some other isolines are drawn. The positions of the open field lines rooted in the photosphere are indicated, as well.

The structure of the magnetic field lines of force was calculated to compare it with the white-light corona form and structures. In doing so, we followed two calculation procedures. In the first one, a regular net of points was chosen at the base of the corona and, then, the open and closed field lines outgoing from this net were traced. Some of the field lines close back to the photosphere and do not reach the source surface, while others rise up to 2.5 $R_\odot$ and spread into interplanetary space. Since the regions of open field lines cover only a small part of the photosphere, the closed field configuration is dominant in the corresponding figures. The resulting pattern may be named the 'upward system'. The open field structure is better illustrated by the second calculation procedure, when the initial net of points is situated at the source surface level (where all field lines are open by definition), and each line is traced down to the photosphere. This pattern may be named the 'downward system'.

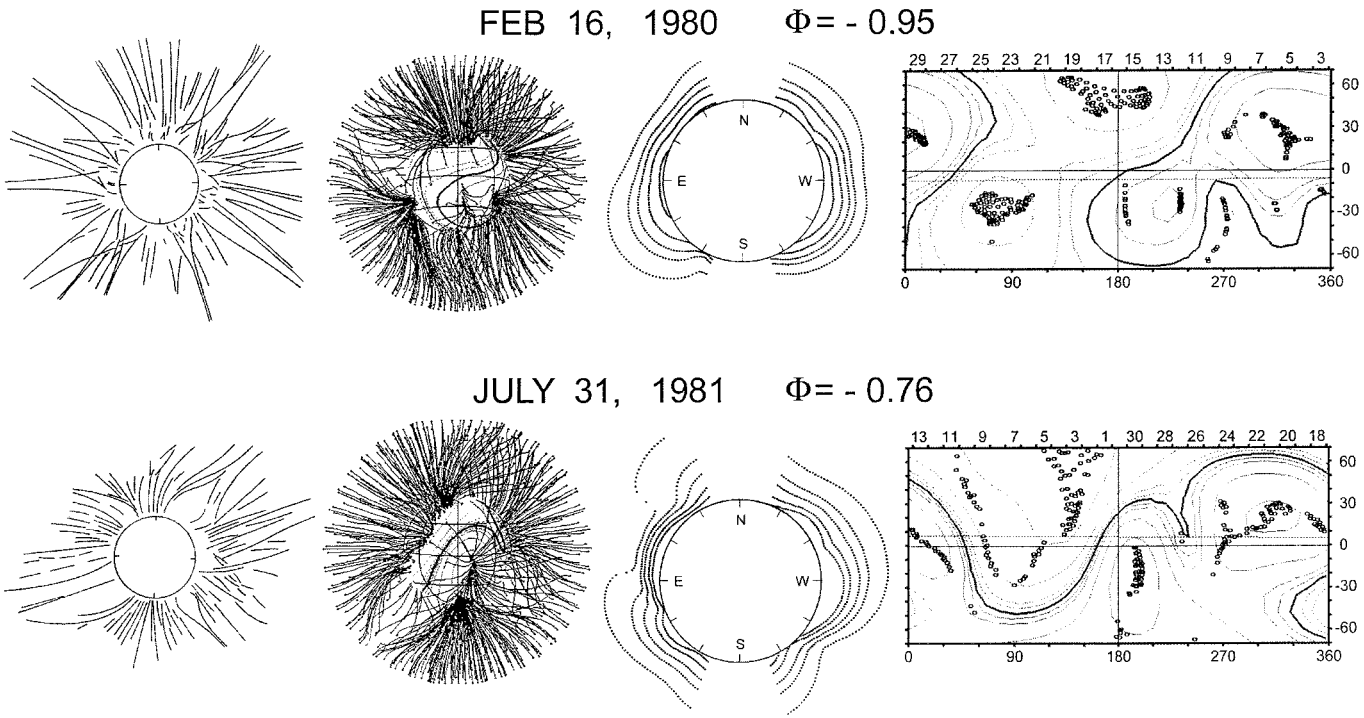

Figure 2. Comparison of the observed white-light corona shapes with the coronal magnetic field topology. The four columns in this figure represent (*from left to right*): drawings of the white-light corona structures; topology of the open field lines; isolines of the magnetic field strength (isogausses); and synoptic charts of the radial magnetic field strength, with the footpoints of the open field lines denoted by *open circles* (the longitudes 90° and 270° represent the solar east and west limbs at the eclipse day). The eclipse dates and the phases in the cycle are given. The eclipses are arranged in the order of increase of their actual phase.

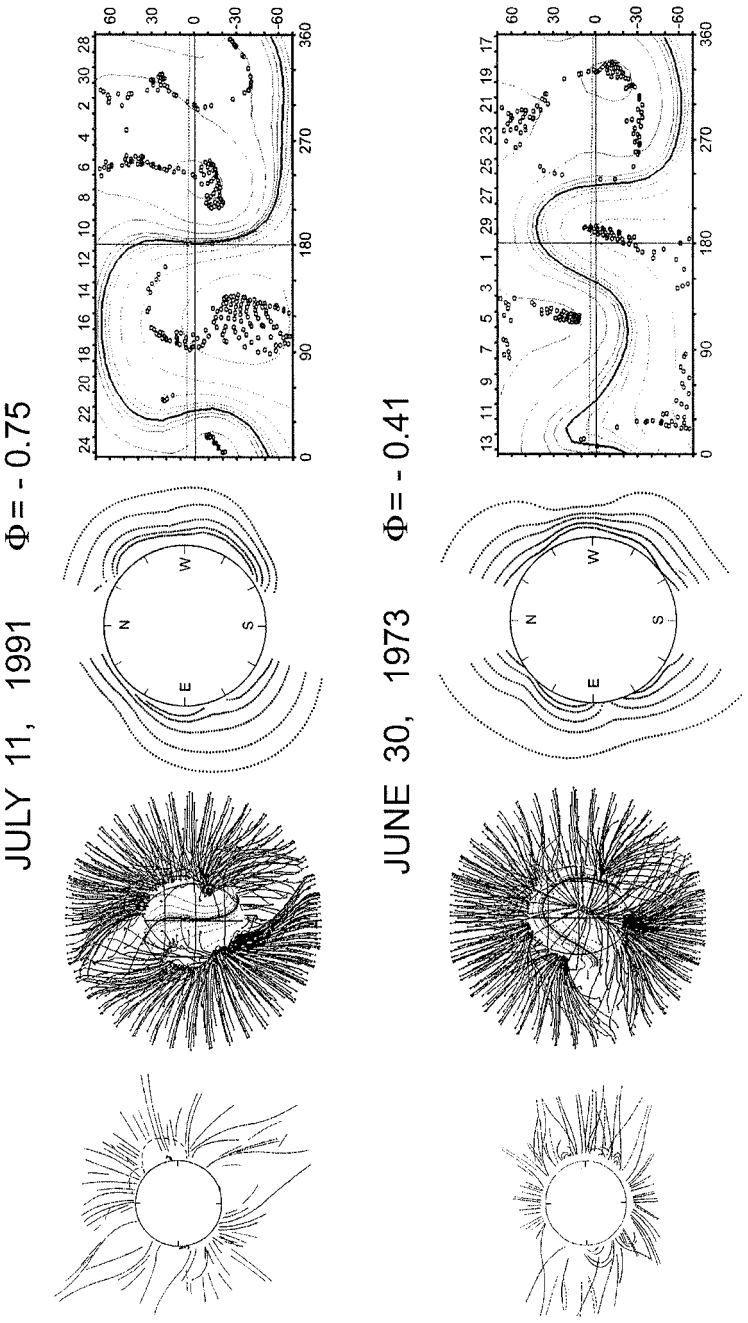

Figure 2. Continued.

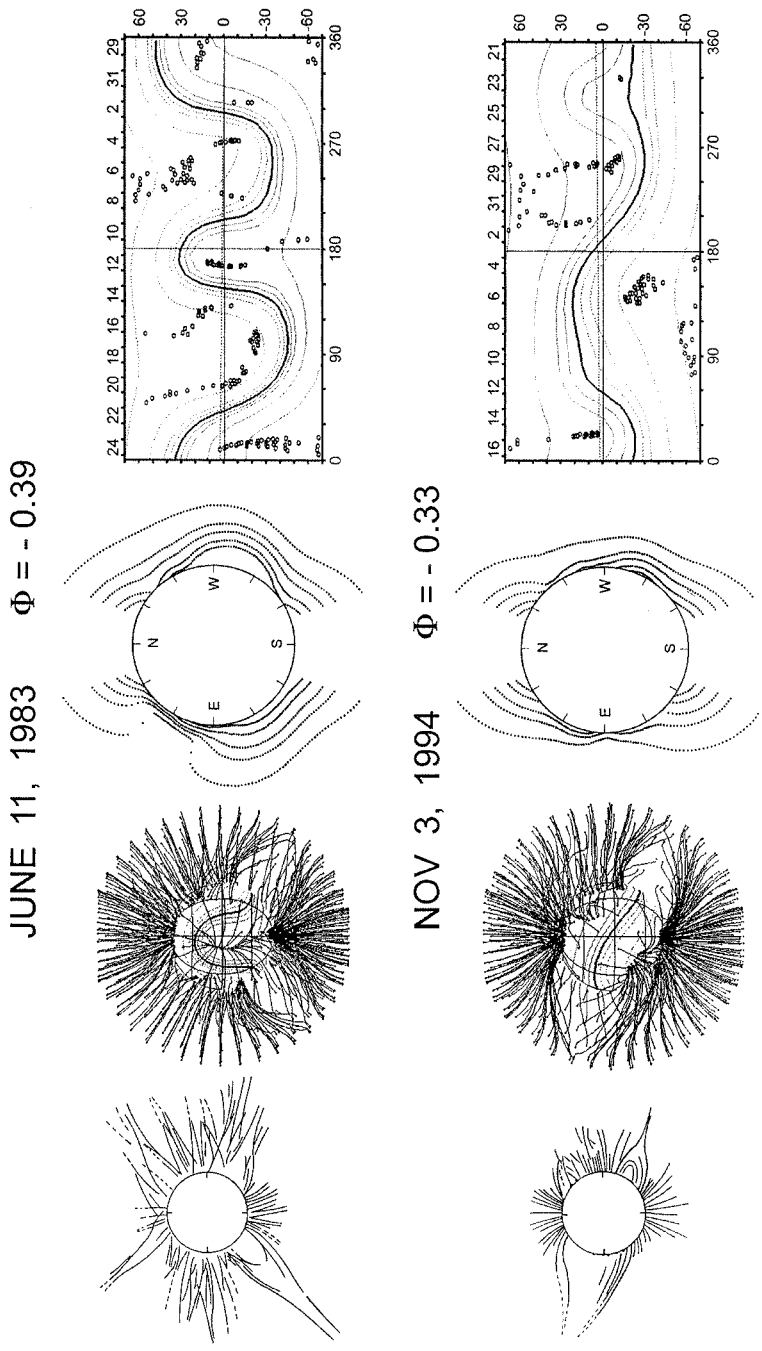

Figure 2. Continued.

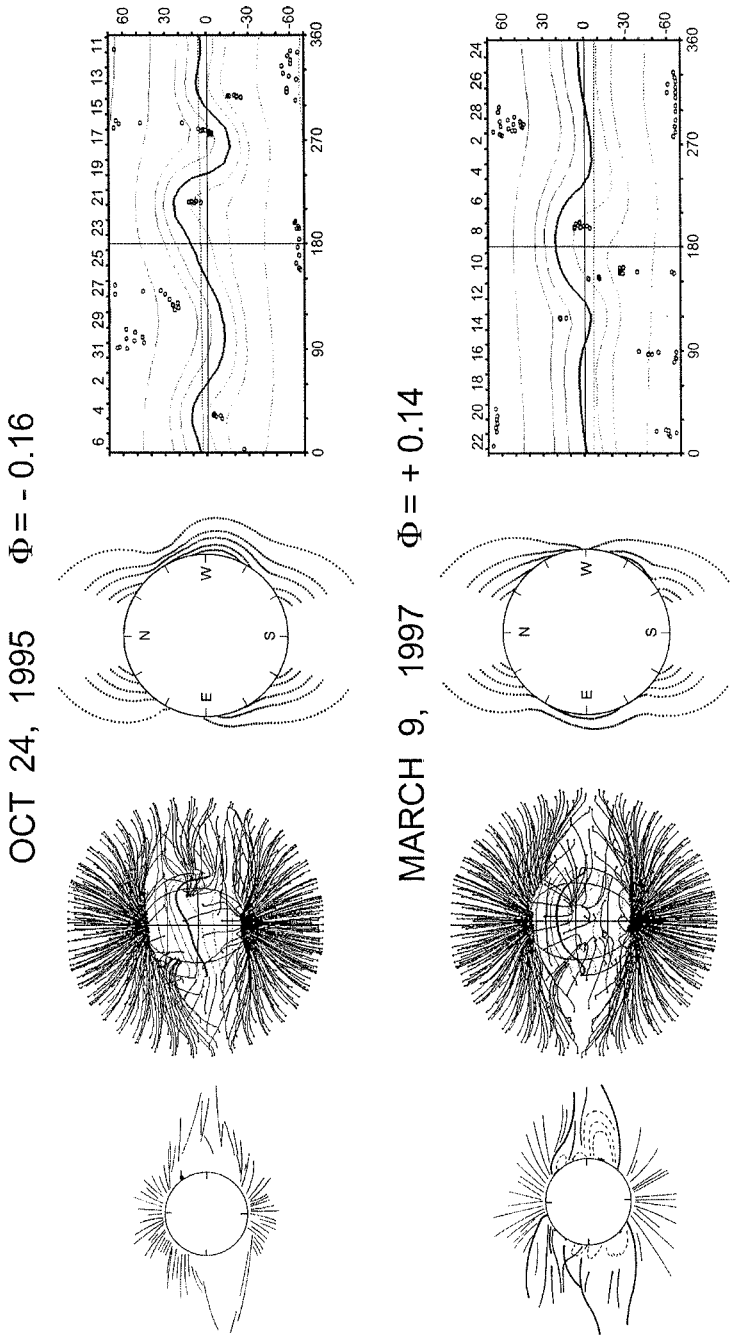

Figure 2. Continued.

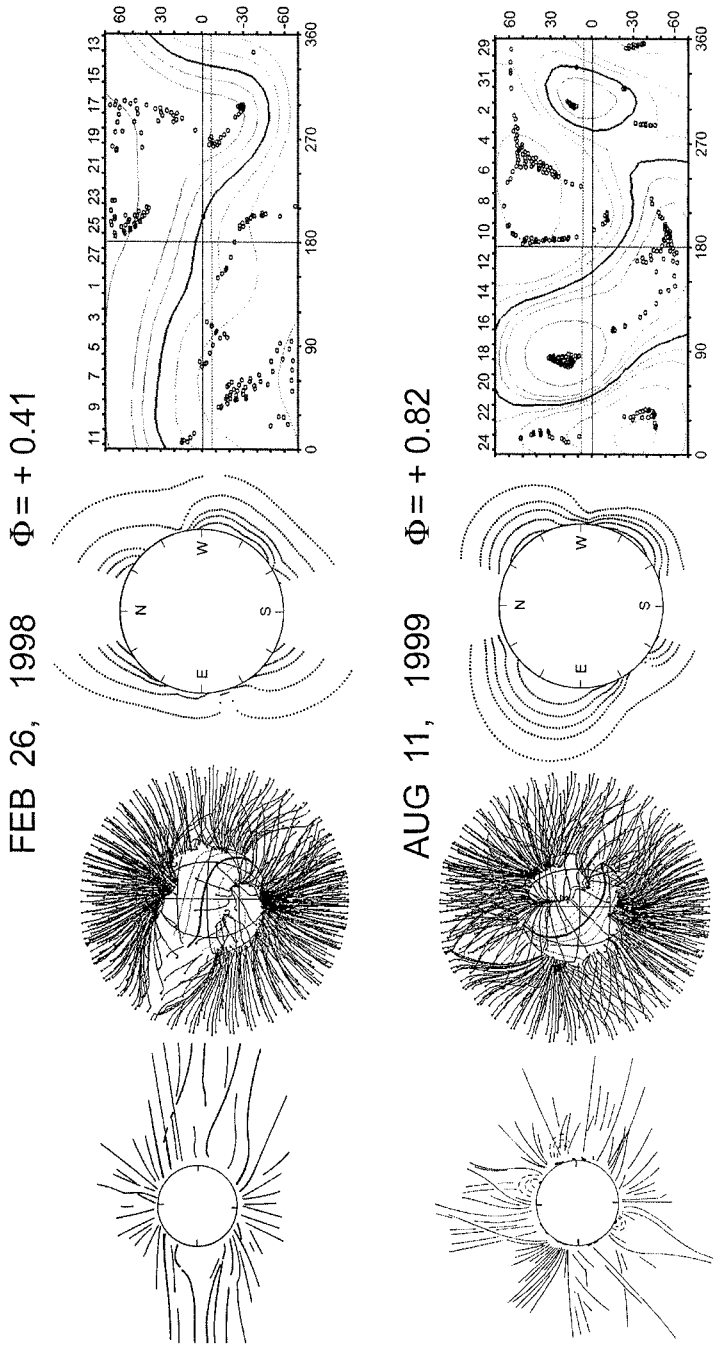

Figure 2. Continued.

3. The Shape of the White-Light Corona and Coronal Magnetic Field

The observed white-light corona shapes and some features of the coronal magnetic field topology are summarized in Figure 2. Here, the eclipses are not arranged chronologically, but according to the increasing phase Φ in the cycle (see Table I). The first column in Figure 2 illustrates individual structural drawings of the corona as obtained by combining negative and positive coronal images and turning them by a small angle. Evolution of the coronal shapes from the flattened minimum corona to the circular maximum corona is well pronounced throughout the solar cycle (for a short discussion on this question, see below). The second column represents the open magnetic field lines of the 'downward system'.

The isolines (so-called isogausses) of the magnetic field strength B are given in the third column in Figure 2. A similar way of representing the magnetic field was earlier used by Gibson and Bagenal (1995) and by ourselves (Sýkora *et al.*, 1999). We do not give isolines above $\pm 70°$, because of the well-known unreliability of magnetic field measurements in the polar zones. The last column in Figure 2 presents the synoptic charts of B with the footpoints of the open field lines identified (small open circles). It should be noted that the synoptic charts are so constructed that the eclipse day falls on the central meridian, i.e., the introduced heliographic longitudes differ from the Carrington longitudes. At the same time, the longitudes 90° and 270° represent the solar east and west limbs at the eclipse day.

Quite a good agreement of the large-scale coronal structures with the coronal magnetic field topology was found for all the ten solar eclipses. Comparison of the first and second columns in Figure 2 reveals that the open magnetic field lines well outline the global coronal shapes observed in 1981, 1991, 1983, 1994, 1997, and 1995. The agreement is also satisfactory for 1980, 1973, and 1999. Only for the 1998 eclipse is the agreement of the two above-mentioned phenomena is somewhat worse. In this particular case, the neutral line of the large-scale magnetic field can be calculated with some uncertainty due to the absence of the Wilcox Solar Observatory measurements in the period from 25 February to 1 March 1998. On the whole, it seems to be proved that the method of the magnetic field calculations applied in our work is well appropriate to describe the basic peculiarities of the coronal global structure. It suggests that, vice versa, the large-scale distribution of the magnetic fields can be deduced, at least qualitatively, by analysing the eclipse white-light corona structures.

In connection with the 1998 eclipse, it is interesting to mention that the corona displayed a surprisingly minimum-like, very flattened global form till late April 1998. Wang, Sheeley, and Rich (2000) explain this unusual situation describing in detail the evolution of the system of coronal streamers and pointing out a sudden reconstruction of their global topology from May 1998 only. Analysis of our magnetic field synoptic charts derived for the source surface level (see also the corresponding charts in *SGD*) confirms that, indeed, the heliospheric current sheet

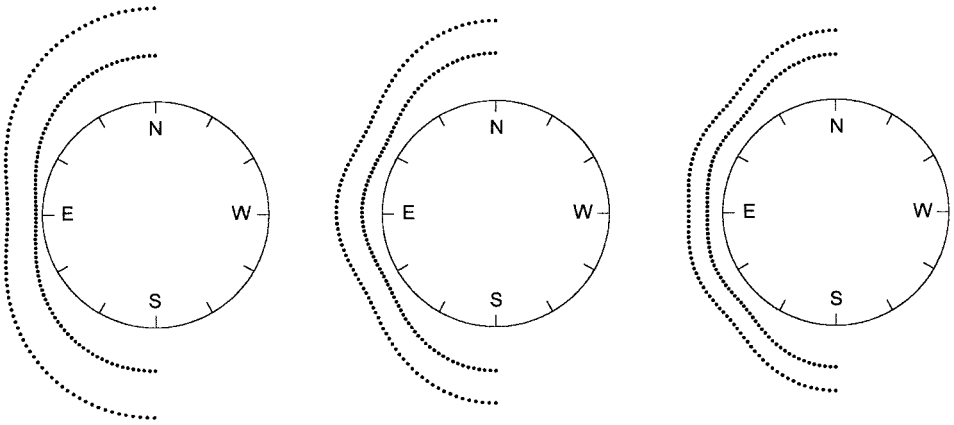

Figure 3. Isolines of the magnetic field strength calculated for the dipole, quadrupole, and octupole (*from left to right*) under the assumption of the magnetic moment equal to 50 μT.

situated in the vicinity of the solar equator was flat from 1996 till August 1997. Its tilt did not exceed 10°–15°. Later, in August–September 1997, the tilt reached 45° and later decreased to 20°–30°. Only in April 1998, the tilt suddenly increased to 60° and more closely approached the values characteristic for the local fields maximum. Though the quasi-maximum form of the corona with some streamers situated close to the solar poles developed rapidly (see the drawing corresponding to the 11 August 1999 eclipse in Figure 2), the most typical maximum corona with a large number of streamers all around the Sun was recorded during the latest 2001 eclipse (not observed by us and not presented here).

The isolines of the magnetic field strength (the third column in Figure 2) are compressed at the magnetic equator and stretched at the magnetic poles. It is particularly well displayed by the minimum type coronae (the eclipses of 1994, 1995, 1997), and also by the unusual corona of 11 July 1991. The latest corona, though related to the close-to-maximum period of the solar cycle, displayed a distinctly minimum-like form, but with the pronounced streamers highly inclined to the heliographic equator. This was, evidently, connected with a large inclination of the global heliomagnetic axis relative to the heliographic axis combined with a specific position of the magnetic equator seen edge-on from the Earth. The combination of these two specific conditions is relatively rare. Correspondingly, the records of the 1991-type coronae are also rare (see Gulyaev and Vanyarkha, 1992).

Considering a certain correspondence between the observed coronal shapes and the coronal magnetic field represented by isolines of B, it is interesting to find out what are the magnetic field harmonics that describe the observed white-light corona forms best of all. In Figure 3, the isolines of B are shown for three basic multipoles – dipole, quadrupole, and octupole. In all these cases, the same value of the magnetic momentum, 50 μT, was adopted in calculations. Figure 3 shows the isolines of B for the eastern hemisphere only. Understandably, the isolines in

the western hemisphere are mirror–symmetrical to the eastern ones. Well-known equations (Hoeksema and Scherrer, 1986; Hoeksema, 1991) have been used to calculate different magnetic field components. For illustration, we give below the equations for determining the radial B_r and longitudinal B_θ components of the field for the cases of simple dipole and quadrupole with the axes identical with the solar rotation axis. In this particular case, the latitudinal component B_φ goes to zero and the full magnetic field strength is $B = \sqrt{B_r^2 + B_\theta^2}$. As in the previous calculations, the source surface radius is equal to 2.5 $R_\odot$. Then, we have for the dipole

$$B_r = g_{10} \cos\theta \left(\frac{2}{r^3} + \frac{1}{2.5^3}\right), \tag{1}$$

$$B_\theta = g_{10} \sin\theta \left(\frac{1}{r^3} - \frac{1}{2.5^3}\right), \tag{2}$$

and for the quadrupole

$$B_r = g_{20} \frac{3\cos^2\theta - 1}{2} \left(\frac{3}{r^4} + \frac{2r}{2.5^5}\right), \tag{3}$$

$$B_\theta = 3\, g_{20} \cos\theta \sin\theta \left(\frac{1}{r^4} - \frac{r}{2.5^5}\right), \tag{4}$$

where g_{10} and g_{20} are the coefficients of the spherically harmonic analysis, corresponding in this particular case to the magnetic moments of the dipole and quadrupole.

Comparison of Figures 2 and 3 indicates that some distributions of isogausses are pretty well described by a single multipole of the global magnetic field. So, for example, the isogauss configurations resemble the dipole distribution close to the minimum of the cycle (1973, 1994, 1995, and 1997 eclipses). The 1991 corona, whose form is similar to that of the cycle minimum, but strongly inclined, may be considered of the same type. The quadrupole component, apparently, contributes considerably to the coronal magnetic field of the 1983 and 1998 eclipses. In some cases, the influence of the next, octupole component is also noticeable. Comparing Figures 2 and 3, one can conclude that, in principle, an adequate combination of the three basic components of the global solar magnetic field can describe the isolines of B of any given eclipse corona. Surely, it is a rather complicated and ambiguous task. It is also clear that the resulting configuration of the magnetic field isolines cannot be obtained by a simple synthesis of the isolines of different multipoles.

Another interesting peculiarity of the magnetic field strength isolines is the presence of moderate bulges at some intervals of the position angles (see, for example, 1983, 1995, and 1999 eclipses). Comparing the positions of these bulges in the system of isogausses with the corresponding synoptic charts, on which the positions of the open field lines outgoing from the base of the corona are drawn,

one can conclude that the bulges (i.e., the regions of increased B) correlate well with the position of the coronal holes situated at the solar limb (see the longitudes 90° and 270° on the synoptic charts) or not far from it. For example, the isogausses of the 1983 eclipse are bulged in the range around the west equator where, on the corresponding synoptic chart, the open circles, indicating the position of the open field lines, are clustered. It was demonstrated earlier (Wang, Howley, and Sheeley, 1996; Obridko and Shelting, 1999b) that the positions of the open field lines indicate, in fact, the presence of coronal holes. A similar situation takes place in the case of the 1995 eclipse.

As for the 1999 corona, a well-expressed bulge in the distribution of the isogausses occurs around the position angle $\sim$ 30°. On the corresponding synoptic chart of the magnetic field, a distinct clustering of the circles is seen at this place at the eastern limb. The drawing of the 1999 corona displays here a plume-like structure, generally typical of the coronal holes. A somewhat less expressive bulge is present in the NW quadrant, the corresponding region on the synoptic chart being at $\sim$ 310°. And finally, a still less distinctive bulge in the SW-quadrant is related to the cluster of circles situated behind the limb.

We should note that similar bulges in the distribution of isogausses are also apparent in Figure 3 in the cases of quadrupole and octupole. It is possible that the appearance of coronal holes, situated at hills of the global magnetic field, is genetically connected with these multipoles. At the same time, the general shape of the solar corona is, first of all, determined by the global dipole. In this case, the extended coronal holes are located around the magnetic poles of the dipole. In the periods of the cycle minima the poles of the dipole and the corresponding coronal holes coincide with the heliographic poles. However, at the particular 1991 eclipse, when the magnetic dipole was strongly inclined, a small coronal hole was recorded close to one of its magnetic poles in the NW quadrant. At the same time, a region with considerably reduced white-light corona brightness and weak green-line emission (both typical of coronal holes) was recorded around the opposite dipole pole (see the structural drawing of this eclipse in Figure 2).

It should be noted that a detailed comparison of the calculated coronal magnetic field with the observed white-light corona structure may be a complementary test for good synthesis of various magnetic field measurements to fit a uniform system of data.

4. Measurements of Coronal Polarization and Magnetic Field

The interesting and somewhat unusual eclipse of 11 July 1991 was already mentioned above. During that eclipse, we obtained images both in the optical continuum and in the coronal green line, together with the polarized images in those spectral ranges (Sýkora and Badalyan, 1992; Badalyan, Livshits, and Sýkora, 1997, 1999). Comparison of the white-light corona isophotes with the isogausses (iso-

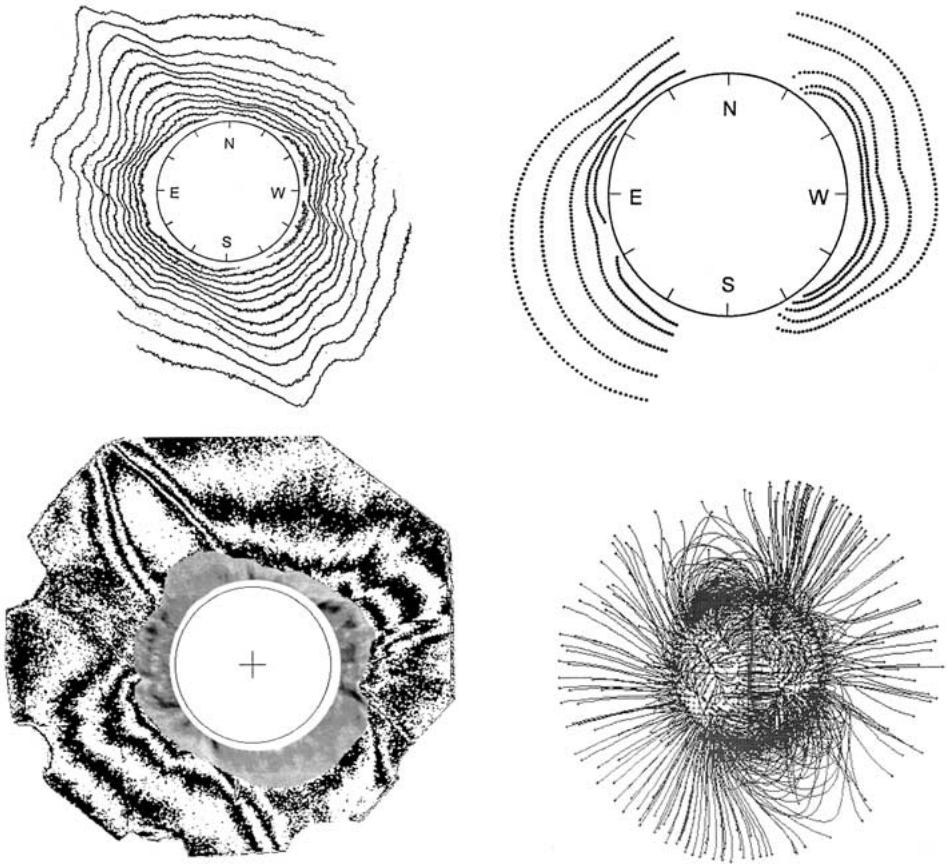

Figure 4. On the upper panels, systems of isophotes (*left*) and isogausses (*right*) and on the lower panels, the coronal structures (*left*) and the structure of the coronal magnetic field 'upward system' (*right*), all derived for the 11 July 1991 eclipse corona, are presented. The middle and outer corona are represented by the polarization chart derived from the polarized white-light corona images, while the structuring of the inner corona (inserted half-tone fragment) is represented by the processed image taken in the coronal green line (see text for details).

lines of B) derived for the 1991 eclipse day (Sýkora *et al.*, 1999) has shown that the isophotes and isogausses form two systems of the mutually perpendicular curves. This is readily seen in Figure 4, two upper panels. For some other eclipses, a similar behaviour was demonstrated by Sýkora, Badalyan, and Obridko (2002).

The polarization measurements made both in the white-light corona and emission coronal lines provide very valuable information about the physical conditions in the corona, first of all, about the coronal density distribution. Particularly, as shown by Badalyan, Livshits, and Sýkora (1993, 1997) and Badalyan and Livshits (1994), the polarization measurements, together with theoretical considerations, make it possible to estimate the coronal matter distribution along the line of sight. For example, high polarization in the well-defined coronal streamers cannot be

interpreted, considering the measured coronal brightness, in terms of spherically symmetric models of the corona: an assumption of a certain concentration of coronal plasma towards the plane of the sky is needed. In quiet regions, such as coronal holes, the assumption of spherical symmetry is valid.

Lower panels in Figure 4 provide a more detailed comparison of the coronal structures (left) with the structures of the magnetic field lines (right) of the 1991 eclipse. We present a combined picture, which allows us to trace the individual coronal structures from the inner corona to its outer layers. In this figure, the structures of the middle and outer corona are visualized by the polarization map, derived from the polarized white-light corona images. The isolines of the degree of polarization (isopleths) are given at a step of 5% by black-and-white gradation. One can clearly see not only the most conspicuous large-scale coronal structures (such as the huge high-latitude streamers and north coronal hole), but also much smaller structural features at the west limb. The inner corona in Figure 4 is presented as a processed image taken through the narrow-band filter $\Delta\lambda = 0.17$ nm in the coronal green line Fe XIV 530.3 nm. Positions of the Sun and its centre during the eclipse are indicated. The innermost layers of the solar corona were covered by the Moon during that long-lasting eclipse.

Figure 4 shows a surprisingly good agreement of the structural features of the inner corona visible in the green-line emission with the structures outlined on the polarization map of the middle and outer white-light corona. One can see how the isopleths trace the boundaries of the huge high-latitude streamers in the NE and SW quadrants, and then, an 'extension' of these lines is continued on the half-tone fragment showing structures in the inner corona. In the region where numerous fine rays are present at low latitudes in the SW quadrant the isopleths form a strongly jagged pattern. On the inner fragment below this pattern, one can see a similar structural feature relevant to the equatorial condensations of the west limb. At the east limb, beside the high-latitude streamer, but closer to the equator, a short bright streamer was observed in the continuum at a position angle of about 60° with a coronal condensation at its base. At this place in Figure 4, we see the form of that streamer marked by isopleths, while in the inner fragment, there is a kind of upper boundary of the coronal condensation turning farther into the boundary of the high-latitude NE-streamer.

Some of the above peculiarities can be identified in the structure of the magnetic field lines. The right lower panel of Figure 4 shows the detailed structure of the magnetic field lines ('upward system', see Section 2). The neutral line calculated for the source surface and projected onto the photosphere at $r = 1.0\ R_\odot$ is drawn. It practically connects the solar poles (see also the synoptic chart in Figure 2). Here, most characteristic features are the arcade of loops over the neutral line and the field lines outlining two systems of the huge helmet streamers in the NE and SW quadrants. One can see that the field lines form high closed loops in the regions of high-latitude streamers, where the isopleths are almost radial. On the contrary, in the regions of equatorial coronal condensations, the closed field lines

reach relatively low heights only, and the isopleths are basically parallel with the limb. These and other peculiarities revealed by comparing the left and right lower panels of Figure 4 demonstrate that polarization observations of the white-light corona can form the basis for further detailed comparison of the white-light corona and coronal magnetic field structures.

5. Conclusions

The white-light corona shapes derived from uniform eclipse observations during 1973–1999 were compared with the variations of the magnetic field global configuration and strength. The topology of the field lines, distribution of the isolines of coronal magnetic field strength B, and field synoptic charts were calculated assuming a current-free character of the field and using mainly the Wilcox Solar Observatory measurements. We show that cyclic variations of the global coronal form agree well with the variations of the global structure of the magnetic field lines in the period under investigation.

The isolines (isogausses) of B are stretched out in the direction of the magnetic poles and compressed in the direction of the magnetic equator. The white-light corona isophotes and the magnetic field isogausses create two systems of closed, mutually perpendicular curves. The characteristic bulges on the isogausses appear in the positions where coronal holes are present on or not far from the limb. In this case, the coronal holes were identified as the regions where the open magnetic field lines are rooted to the photosphere. We calculated the isogausses for the basic harmonics of the global magnetic field – the dipole, quadrupole, and octupole. Various combinations of these multipoles allow us, in principle, to describe any global coronal structure observed.

Almost perfect correspondence exists between the individual white-light corona structures and the features of the closed magnetic field lines. The structures seen in the middle and outer white-light corona are well-outlined by the isopleths (the lines of equal degree of polarization), while the structures of the inner corona are noticeable on the processed image taken in the light of the Fe XIV 530.3 nm emission coronal line. Exceptionally good agreement of the inner 'green-line' structures with the middle and outer 'white-light' ones was revealed.

The well-known coronal flattening dependence on the phase in the solar cycle seems to be seriously questioned during the last decade. We, and some other authors (Gulyaev, 1992, 1994; Sýkora and Badalyan, 1992; Sýkora *et al.*, 1998, 1999), are of opinion that the Ludendorff's definition of the solar corona flattening (Ludendorff, 1928) and the generally accepted variations of the coronal forms during the solar cycle (see, e.g., Golub and Pasachoff, 1997) are to a large extent fictitious. In fact, the solar corona is very likely to always be considerably flattened, but this flattening is rather towards the solar magnetic equator than towards the

heliographic equator. However, the calculation of the coronal flattening ε using the magnetic field data is a separate, not easy problem.

The comparison of the global white-light corona structures with the magnetic field parameters (structure of the field lines, distribution of the magnetic field strength isolines, and B_r synoptic charts) has shown their good mutual correspondence. Therefore, it is believed that white-light corona eclipse observations performed for more than a century could provide information on the long-term evolution of the solar global magnetic field. In this context, a careful investigation of the eclipse descriptions in the old chronicles could be also informative for understanding the solar magnetic field variations far before the rise of solar physics and measurements.

Acknowledgements

The authors greatly appreciate the support of the VEGA Grant 2/1022/21 of the Slovak Academy of Sciences, and Grants No. 02-02-16199 of the Russian Foundation for Basic Research and INTAS 2000-840. We are grateful to Wilcox Solar Observatory staff for the solar magnetic field data and to T. Pintér from Hurbanovo Observatory (Slovakia) for collaboration in observations during the eclipses Nos. 6-8 (see Table I).

References

Badalyan, O. G. and Livshits, M. A.: 1994, in V. Rušin, P. Heinzel, and J.-C. Vial (eds.), *Solar Coronal Structures*, Veda Bratislava, p. 77.

Badalyan, O. G. and Sýkora, J.: 1997, *Astron. Astrophys.* **319**, 664.

Badalyan, O. G., Livshits, M. A., and Sýkora, J.: 1993, *Solar Phys.* **145**, 279.

Badalyan, O. G., Livshits M. A., and Sýkora J.: 1997, *Solar Phys.* **173**, 67.

Badalyan, O. G., Livshits, M. A., and Sýkora, J.: 1999, *Astron. Astrophys.* **349**, 295.

Badalyan, O. G., Obridko, V. N., and Sýkora, J.: 2002a, *Contrib. Astron. Obs. Skalnaté Pleso* **32**, 49.

Badalyan, O. G., Obridko, V. N., and Sýkora, J.: 2002b, *Contrib. Astron. Obs. Skalnaté Pleso* **32**, 175.

Gelfreikh, G. B., Pilyeva, N. A., and Ryabov, B. I.: 1997, *Solar Phys.* **170**, 253.

Gibson, S. E. and Bagenal, F.: 1995, *J. Geophys. Res.* **100**, 19865.

Golub, L. and Pasachoff, J. M.: 1997, *The Solar Corona*, Cambridge University Press, Cambridge, p. 110.

Grebinskij, A., Bogod, V., Gelfreikh, G., Urpo, S., Pohjolainen, S., and Shibasaki, K.: 2000, *Astron. Astrophys. Suppl.* **144**, 169.

Gulyaev, R. A.: 1992, *Solar Phys.* **142**, 213.

Gulyaev, R. A.: 1994, *Astrophys. J.* **437**, 867.

Gulyaev R. A. and Vanyarkha, N. Ya.: 1992, *Solar Phys.* **140**, 369.

Hoeksema, J. T.: 1991, *Solar Magnetic Fields – 1985 through 1990*, Report CSSA-ASTRO-91-01.

Hoeksema, J. T. and Scherrer, P. H.: 1986, *The Solar Magnetic Field – 1976 through 1985*, WDCA Report UAG-94, NGDC, Boulder.

Ivanov, K. G. and Kharshiladze, A. P.: 1994, *Geomagn. Aeron.* **34**, 22.

Loucif, M. L.: 1988, in R. C. Altrock (ed.), *Solar and Stellar Coronal Structure and Dynamics*, Sunspot, NM, p. 406.
Loucif, M. L. and Koutchmy, S.: 1989, *Astron. Astrophys. Suppl.* **77**, 45.
Ludendorff, H.: 1928, *Sitzber. Preuss. Akad. Wiss.* **16**, 185.
Mitchell, S. A.: 1929, *Handb. Aph.* **4**, 231.
Obridko, V. N. and Shelting, B. D.: 1999a, *Solar Phys.* **184**, 187.
Obridko, V. N. and Shelting, B. D.: 1999b, *Solar Phys.* **187**, 185.
Sýkora, J. and Badalyan, O. G.: 1992, in C. Mattok (ed.), *Coronal Streamers and Coronal Loops and Solar Wind Composition*, ESA, SP-348, p. 137.
Sýkora, J., Badalyan, O. G., and Obridko, V. N.: 2002, *Adv. Space Res.* **29**, 395.
Sýkora, J., Ambrož, P., Minarovjech, M., Obridko, V. N., Pintér, T., and Rybanský, M.: 1998, *Solar Jets and Coronal Plumes*, ESA, SP-421, p. 79.
Sýkora, J., Badalyan, O. G., Obridko, V. N., and Pintér, T.: 1999, *Contrib. Astron. Obs. Skalnate Pleso* **29**, 89.
Vasil'eva, V. V.: 1998, in V. I. Makarov and V. N. Obridko (eds.), *Novy tsikl aktivnosti Solntsa: nablyudatelny i teoretichesky aspekty*, St.-Peterburg, p. 213.
Vasil'eva, V. V. and Tlatov, A. G.: 2002, private communication.
Vsekhsvyatsky, S. K., Nikolsky, G. M., Ivanchuk, V. I., Nesmyanovich, I. A., Ponomarev, E. A., Rubo, G. A., and Cherednichenko, V. I.: 1965, in S. K. Vsekhsvyatsky (ed.), *Solar Corona and Corpuscular Emission in the Interplanetary Space*, Kiev University Publ. House, Kiev, p. 73 (in Russian).
Wang, Y.-M., Hawley, S. H., and Sheeley, N. R., Jr.: 1996, *Science* **271**, 417.
Wang, Y.-M., Sheeley, N. R., Jr., and Rich, N. B.: 2000, *J. Geophys. Res. Lett.* **27**, 149.